NANO LETTERS

2002
Vol. 2, No. 5
513−517

Hexagonal Pore Organization in Mesostructured Metal Tin Sulfides Built with $[Sn_2S_6]^{4-}$ Cluster

Krishnaswamy K. Rangan, Pantelis N. Trikalitis, Christian Canlas, Thomas Bakas,† David P. Weliky, and Mercouri G. Kanatzidis*

Department of Chemistry, Michigan State University, East Lansing, Michigan 48824 and Department of Physics, University of Ioannina, Ioannina, 45110, Greece

Received January 4, 2002; Revised Manuscript Received February 18, 2002

ABSTRACT

We present the first report of hexagonally ordered mesostructured ternary metal tin sulfide materials along with their structure and optical properties. The new mesophases designated as $(CP)_xM_ySn_2S_6$ ($M = Zn^{2+}$, Cd^{2+}, Ga^{3+}) where synthesized by linking $[Sn_2S_6]^{4-}$ clusters with metal ions in the presence of cetylpyridinium (CP) surfactant molecules in formamide solution under basic conditions. The materials are semiconductors in the energy range $2.5 < E_g < 3.1$ eV. The mesostructured $(CP)_xM_ySn_2S_6$ show photoluminescence, when excited with light above the band gap.

Non-oxidic materials with open frameworks and designed pore structures are highly attractive because of the potential impact in areas such as photocatalysis, adsorption, sensing, photonics and electroluminescence.[1] Semiconducting mesostructured materials with ordered pores may produce a periodic array of "antidots", a structure geometrically complementary to a quantum-dot array, consisting of continuous semiconductor space separated by dielectric voids.[2] Despite significant advances in the design and synthesis of mesostructured silicates,[3] the construction of non-silicate analogues,[4] especially chalcogenides, presents considerable challenge partly because of the unstable precursor anions and poor understanding of their condensation behavior in solution. However, this area also represents greater opportunities because of the potentially large variety of building blocks and types of materials that can be prepared. Recently mesostructured metal germanium chalcogenides based on $[Ge_4Q_{10}]^{4-}$ (Q = S, Se) clusters with hexagonal ordered and worm-hole type pore structures were reported.[5,6] Three-dimensional ordered mesostructured tin sulfides, on the other hand, have not been investigated, although syntheses of meso-lamellar tin sulfides have been reported.[7] We adopted a coordination self-assembly approach to construct new phases with anionic tin sulfide clusters and present here the first description of hexagonally ordered mesostructured metal tin sulfide materials.

Initially, we employed the simple tetrahedral $[SnS_4]^{4-}$ anion the sulfide analogue of $[SnSe_4]^{4-}$.[8] To our surprise the chemistry of this simple $[SnS_4]^{4-}$ species turned out to be very different from that of its selenide version. Syntheses involving Na_4SnS_4 and formamide (FM) as a solvent yielded highly disordered phases with irreproducible compositions. This unanticipated difficulty prompted us to investigate the reasons for this behavior. We discovered that the stability of $[SnS_4]^{4-}$ is dependent on the pH and nature of solvent.[9] This was determined from solution ^{119}Sn nuclear magnetic resonance (NMR) experiments in water and FM,[10] which showed that in water $[SnS_4]^{4-}$ maintains its integrity, whereas in FM it converts to the dimeric cluster according to the eq 1.

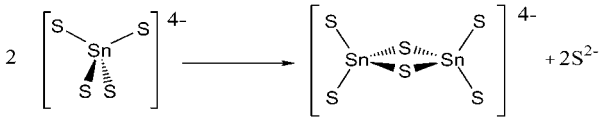

(1)

This process never identified before in FM, greatly complicated efforts to use $[SnS_4]^{4-}$ as a precursor. In the face of this new information, we selected the more stable $[Sn_2S_6]^{4-}$ anion itself and found it to be an excellent precursor to ordered mesostructured sulfide materials.

Indeed, the new mesophases $(CP)_xM_ySn_2S_6$ ($M = Zn^{2+}$, Cd^{2+},Ga^{3+}) were synthesized by the addition of a solution of metal cations to the FM solution of supramolecularly organized $[Sn_2S_6]^{4-}$ dimers templated with cetylpyridinium (CP) molecules. It was required to use basic solutions (pH > 9), by dissolving ammonia in FM, to avoid precipitation of SnS_2 during the reaction. EDS analysis also indicated that no chlorine, bromine or sodium was present in the materi-

† Department of Physics, University of Ioannina.

10.1021/nl025502k CCC: $22.00 © 2002 American Chemical Society
Published on Web 03/19/2002

Table 1. Band Gaps, Elemental Analyses, TGA Analyses, and Powder XRD Data of $(CP)_xM_ySn_2S_6$ Phases

mesophase	band gap/eV (color)	C,H,N analyses (%)	TGA wt. loss (%)	atom ratio M:Sn:S	powder XRD data/*d* (Å)
$(CP)_{1.4}Zn_{1.3}Sn_2S_6$	3.0 (pale white)	34.9, 6.0, 3.1	45.2	1.3:2:5.8	35.3, 20.1
$(CP)_{1.2}Cd_{1.4}Sn_2S_6$	2.5 (yellow)	33.2, 5.9, 2.9	44.3	1.4:2:5.8	36.1, 19.2
$(CP)_{1.1}Ga_{0.9}Sn_2S_6$	3.1 (light yellow)	30.1, 5.8, 3.8	43.5	0.9:2:5.6	34.4, 18.8

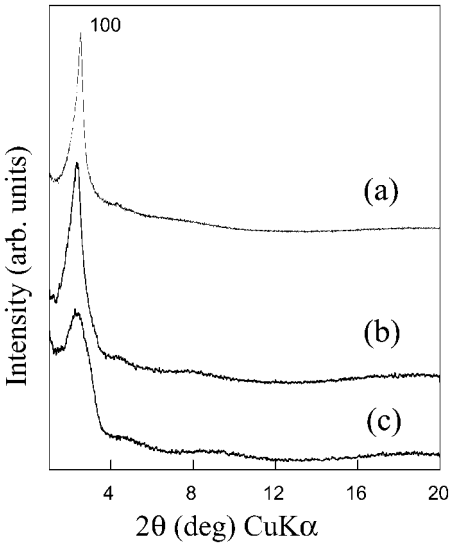

Figure 1. X-ray diffraction patterns of (a) $(CP)_{1.4}Zn_{1.3}Sn_2S_6$, (b) $(CP)_{1.2}Cd_{1.4}Sn_2S_6$, and (c) $(CP)_{1.1}Ga_{0.9}Sn_2S_6$. The diffraction patterns were recorded on a Rigaku diffractometer using CuKα radiation.

als.[11] Infrared spectroscopy confirmed the presence of cetylpyridinium ions. A summary of the analytical and other data is given in Table 1.[12]

Powder X-ray diffraction (XRD) patterns of the $(CP)_xM_y$-Sn_2S_6 (M= Zn^{2+}, Cd^{2+}, Ga^{3+}) phases show a strong peak at low scattering angles (*d* value ≈ 35 Å) corresponding to (100) reflections (Figure 1), followed by a broad peak at 4−5°. The latter could correspond to the overlapping higher-order (110) and (200) reflections of the hexagonal lattice as observed by transmission electron microscopy (TEM). These peaks are not well resolved possibly due to broadening associated with small particle sizes. The lack of high angle Bragg diffraction peaks indicates an amorphous nonperiodic character of the inorganic wall very similar to the one of mesostructured silica MCM-41.[13]

Direct observation of the local organization of the pores was accomplished by TEM. Figure 2a shows a characteristic TEM image of $(CP)_{1.4}Zn_{1.3}Sn_2S_6$, down the pore tunnel axis where the hexagonal structure is clearly visible. Figure 2b shows tubular arrangement of pores filled with rod like surfactant micelles, perpendicular to pore tunnel axis. The pore-pore distances observed in the TEM images are in the range ∼38−40 Å and agree well with the values obtained from the XRD data. The particles possess morphologies with relatively sharp edges (Figure 2c). The hexagonal symmetry of the pores was further exemplified convincingly, by electron diffraction patterns observed from the particles. The insert in Figure 2a shows the electron diffraction pattern of $(CP)_{1.4}Zn_{1.3}Sn_2S_6$ with hexagonal indexing of the diffraction spots. The observed d_{100} value of 39 Å from the electron diffraction pattern is close to the value observed from powder XRD pattern (Table 1).

The materials display strong diffuse scattering which can be analyzed to probe the local structure of the amorphous metal tin sulfide framework (i.e., the walls). Namely, the high angle X-ray diffuse scattering was used to compute the atom pair distribution function (PDF) which essentially reveals all the correlated interatomic vectors in the structure.[14] Figure 3 shows the reduced structure factor, Q[S(Q)-1], of $(CP)_{1.4}Zn_{1.3}Sn_2S_6$ obtained from the powder diffraction data and the corresponding PDFs. The PDF shows

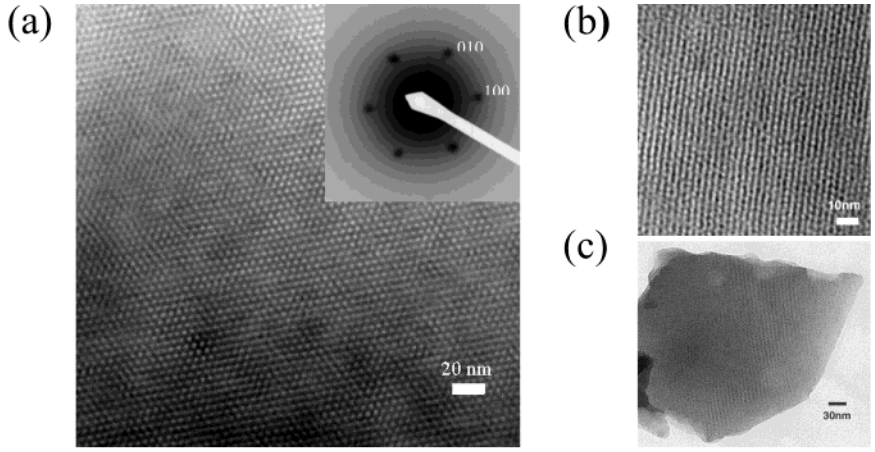

Figure 2. TEM images of $(CP)_{1.4}Zn_{1.3}Sn_2S_6$ (a) parallel to pore axis (insert shows corresponding electron diffraction pattern, *hk*0 zone), (b) view perpendicular to pore axis, and (c) large particle of $(CP)_{1.3}Zn_{1.3}Sn_2S_6$ material. TEM was performed with a JEOL 120 CX operating at 120 kV using carbon supported copper grids dipped in a suspension of the sample in ether.

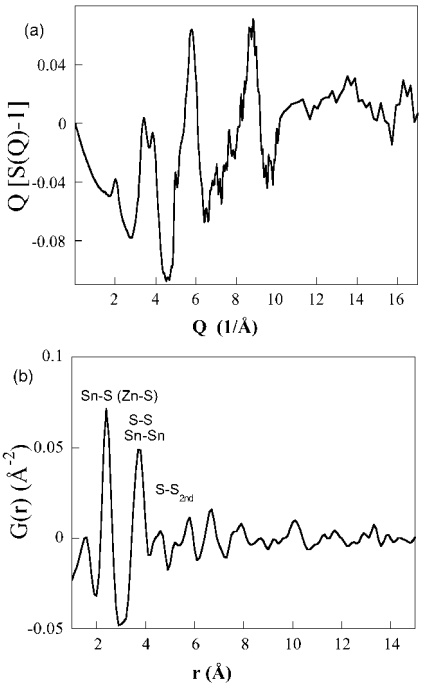

Figure 3. (a) Reduced structure factors Q[S(Q)-1] for $(CP)_{1.4}Zn_{1.3}Sn_2S_6$ (b) Reduced pair distribution function, *G(r)* showing all interatomic vectors in the structure. The labeled peaks are interatomic pair correlations associated with the presence of the metal linked $[Sn_2S_6]^{4-}$ clusters. The XRD data for the pair distribution function (PDF) determination were collected independently using a Huber diffractometer in a symmetric reflection geometry and AgKα radiation.

a well-defined local order as seen by the presence of strong inter atomic correlation vectors at 2.4 and 3.8 Å, which correspond to Sn−S (and Zn−S) and S−S distances in the $[Sn_2S_6]^{4-}$ dimer. Further, there is no observable structural coherence above 8 Å because of the lack of well-defined orientational relationship between the neighboring $[Sn_2S_6]^{4-}$ dimers.

Solid state ^{119}Sn NMR spectroscopy gave further insight into the local coordination and oxidation state of Sn present in these mesophases.[15] Figure 4a shows the ^{119}Sn magic angle spinning (MAS) NMR spectrum of $(CP)_{1.4}Zn_{1.3}Sn_2S_6$. The spectrum consists of a single isotropic, relatively narrow resonance at 74.5 ppm and spinning sidebands of this resonance, indicating that all Sn sites have approximately the same local environment. The observed chemical shift is consistent with tetrahedrally coordinated Sn rather than five or six coordinated.[16] Despite the high spinning rates used, an extensive array of spinning sidebands extending over ~300 ppm was observed, which shows that there is a substantial chemical shift anisotropy (CSA) in the mesophase as observed for $[Sn_2S_6]^{4-}$ clusters.[17] By comparison Na_4SnS_4, where totally symmetric $[SnS_4]^{4-}$ anions are present, no spinning sidebands were observed consistent with small CSA.

^{119}Sn Mössbauer spectroscopy was used to confirm the oxidation state of tin in the $(CP)_xM_ySn_2S_6$ phases.[18] Figure 4b shows the Mössbauer spectrum for $(CP)_{1.4}Zn_{1.3}Sn_2S_6$ and can be fitted well with a set of two overlapping quadrupole doublets (isomer shift, δ, and quadrupole splitting, ΔE_q parameters, 1.20/1.13 (37%), 1.20/1.46 (63%)). The isomer shift values are consistent with Sn^{4+}. The presence of two quadrupole doublets indicates that there are at least two different binding modes of $[Sn_2S_6]^{4-}$ in the mesophase.

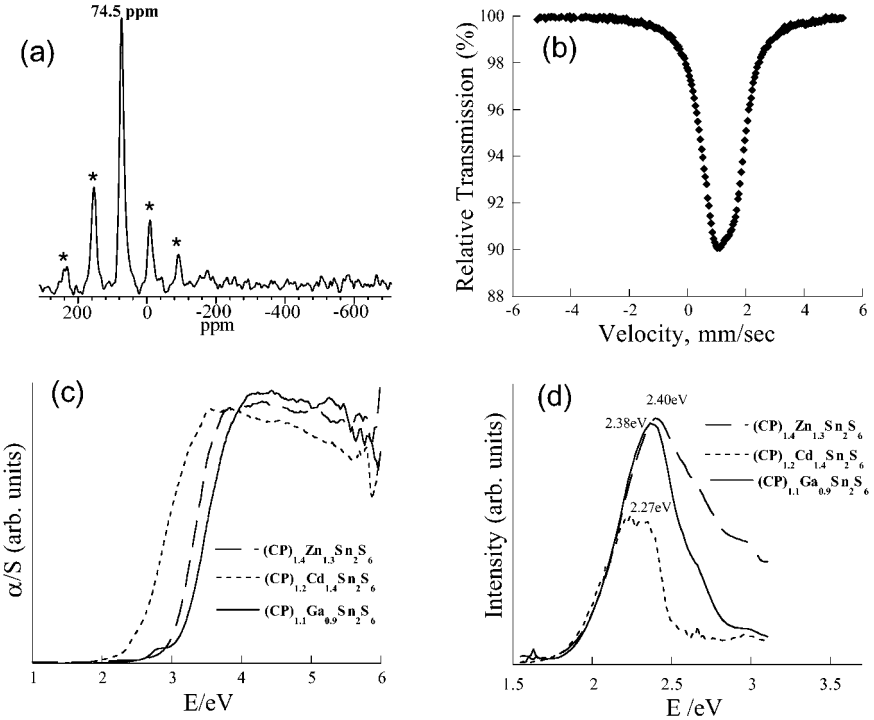

Figure 4. (a) Solid state ^{119}Sn NMR spectrum of $(CP)_{1.4}Zn_{1.3}Sn_2S_6$ at room temperature. The peaks marked with a ∗ are spinning sidebands. (b) Mössbauer spectrum of $(CP)_{1.4}Zn_{1.3}Sn_2S_6$ at 85 K. ^{119}Sn Mössbauer spectra were obtained using a constant acceleration spectrometer with a 5mCi $CaSnO_3$ source kept at room temperature. The isomer shift values are given relative to $CaSnO_3$. (c) Room-temperature solid-state optical absorption spectra. Optical absorption spectra were obtained at 300 K with a Shimadzu UV-3101PC double beam, double monochromator spectrophotometer equipped with an integrating sphere. (d) photoluminescence spectra of $(CP)_xM_ySn_2S_6$ ($M = Zn^{2+}$, Cd^{2+}, Ga^{3+}). PL spectra were obtained on a Spex Fluorolog-2 F111A1 spectrofluorimeter.

Optical absorption spectra of $(CP)_xM_ySn_2S_6$ show well-defined semiconductor band gaps, E_g, (Figure 4c and Table 1), lying between those of ZnS(3.6 eV) and ZnSe(2.6 eV). The E_g values vary with the metal ions linking the $[Sn_2S_6]$ dimers in the order $Ga^{3+} > Zn^{2+} > Cd^{2+}$. The metal tin sulfide phases reported here possess lower band gap than the corresponding Ge_4S_{10}-based systems. For example, CPZnGeS has a band gap of 3.4 eV as compared to 3.0 eV for $(CP)_{1.4}Zn_{1.3}Sn_2S_6$.

In addition, the metal tin sulfide mesophases show intense photoluminescence, similar to metal germanium sulfide mesophases,[19] when excited with light above the band gap, Figure 4d. With an excitation line of 3.3 eV (390 nm) intense green emission was observed at 77K for $(CP)_{1.4}Zn_{1.3}Sn_2S_6$ with a maximum at 2.4 eV. The emission maxima for Ga and Cd analogues were 2.38 and 2.27 eV respectively, which are similar to those observed for the corresponding metal Ge_4S_{10}-based phases (e.g., 2.35 eV for CPGaGeS).[19] The surfactant CPBr alone emits at much higher energy 2.87 eV. The origin of PL is most likely the pyridinium chromophore of the surfactant because similar mesostructured M/Sn_2S_6 materials synthesized with the cetyltrimethylammonium surfactant[20] ($C_{16}H_{33}NMe_3Br$) did not show PL at the same temperature. It is interesting to note that light emission was observed even with excitation energies below the $\pi-\pi^*$ transition of pyridinium (3.62 eV). Accordingly, both surfactant and inorganic framework are required for the observed PL. This demonstrates that interesting properties can derive from the presence of the surfactants themselves in these mesophases and from the interaction of these surfactants with the semiconducting inorganic framework. In this context, the materials reported here could be considered to be true organic−inorganic nanocomposites.

Experimental Section

In a typical synthesis, a solution of 4 g (10 mmol) of surfactant ($CPBr\cdot H_2O$) in 10 mL of FM was heated at 70 °C for a few minutes forming a clear solution. Then ammonia was bubbled through the solution to increase the pH ∼9. To this solution 0.6 g (1 mmol) of $Na_4Sn_2S_6\cdot 14H_2O$ in 10 mL of FM at 70 °C was added to form a clear yellow solution. To this solution a FM solution of 1 mmol of the metal chloride was added dropwise. A precipitate formed immediately and the mixture was stirred at 70 °C for 24 h. The products were isolated by filtration and washed copiously with warm FM and water. The solids were dried under vacuum. The yields were ∼90% in all cases based on $Na_4Sn_2S_6\cdot 14H_2O$.[21]

The solution ^{119}Sn NMR spectra were recorded at 186.4 MHz on a Varian VXR500 spectrometer in a coaxial 5 mm tube at 300 K. The solid-state spectra were taken at room temperature on a 400 MHz Infinity Plus 400 NMR Spectrometer using a double resonance MAS probe with proton decoupling. Samples were spun using zirconia rotors of 4 mm. o.d. at the speed of 12−13 kHz. For ^{119}Sn, a spectral frequency of 148.6 MHz, a 90° pulse length of 2 μs, and a relaxation delay of 70s was used. In these spectra the detection channel was tuned to ^{119}Sn. All spectra are referenced with respect to Me_4Sn.

Acknowledgment. Financial support from the National Science Foundation (CHE-99−03706, Chemistry Research Group) is gratefully acknowledged. This work made use of SEM and TEM facilities of the Center for Advanced Microscopy at Michigan State University.

References

(1) Ozin, G. A. *Materials Chemistry, An Emerging Subdiscipline, Adv. Chem. Ser*.; Interrante, L., Ed. **1995**, *245*, 335−372. Barton, T. J.; Bull, L. M.; Klemperer, W. G.; Loy, D. A.; McEnaney, B.; Misono, M.; Monson, P. A.; Pez, G.; Scherer, G. W.; Vartuli, J. C.; Yaghi, O. M. *Chem. Mater*. **1999**, *11*, 2633−2656. Axtell, A. E.; Liao, J. H.; Pikramenou, Z.; Park, Y.; Kanatzidis, M. G. *J. Am. Chem. Soc*. **1993**, *115*, 12 191.

(2) Weiss, D.; Roukes, M. L.; Menschig, A.; Grambow, P. *Nanostructures and Mesoscopic Systems*; Kirk, W. P., Reed, M. A., Eds.; Academic Press: Boston; 1992, pp 299−309. Turton, R. *The Quantum Dot*; Oxford University Press: New York, 1995. Bowes, C. L.; Ozin, G. A. *Mater. Res. Soc. Symp. Proc*. **1993**, *286*, 93−98.

(3) Ciesla, U.; Schüth, F. *Microporous Mesoporous Mater*. **1999**, *27*, 131.

(4) Schüth, F. *Chem. Mater*. **2001**, *13*, 3184.

(5) MacLachlan, M. J.; Coombs, N.; Ozin, G. A. *Nature* **1999**, *397*, 681−684. MacLachlan, M. J.; Coombs, N.; Bedard, R. L.; White, S.; Thompson, L. K.; Ozin, G. A. *J. Am. Chem. Soc.* **1999**, *121*, 12 005−12 017.

(6) Rangan, K. K.; Billinge, S. J. L.; Petkov, V.; Heising, J.; Kanatzidis, M. G. *Chem. Mater*. **1999**, *11*, 2629−2632. Wachhold, M.; Rangan, K. K.; Lei, M.; Thorpe, M. F.; Billinge, S. J. L.; Petkov, V.; Heising, J.; Kanatzidis, M. G. *J. Solid State Chem.* **2000**, *152*, 21−36.

(7) Li, J. Q.; Kessler, H.; Delmotte, L. *J. Chem. Soc.-Faraday Trans.* **1997**, *93*, 665−668. Li, J. Q.; Kessler, H. *Microporous Mater*. **1997**, *9*, 141−147. Li, J. Q.; Delmotte, L.; Kessler, H. *Chem. Commun.* **1996**, 1023−1024. Jiang, T.; Ozin, G. A. *J. Mater. Chem.* **1997**, *7*, 2213−2222. Li, J. Q.; Marler, B.; Kessler, H.; Soulard, M.; Kallus, S. *Inorg. Chem.* **1997**, *36*, 4697−4701.

(8) Trikalitis, P. N.; Rangan, K. K.; Bakas, T.; Kanatzidis, M. G. *Nature* **2001**, *410*, 671.

(9) Krebs, B. *Angew. Chem., Int. Ed. Engl*. **1983**, *22*, 113.

(10) The NMR spectra of $Na_4SnS_4\cdot 14H_2O$ and $Na_4Sn_2S_6\cdot 14H_2O$ in FM are identical showing a single resonance at 53 ppm (relative to Me_4Sn), whereas in water they are different, showing a single line at 69 ppm and 55 ppm, respectively.

(11) The elemental composition was determined by energy-dispersive microprobe analysis (EDS), elemental C, H, N and thermogravimetric analysis (TGA). In all samples the ratio of Sn:S was close to 1:3 in agreement with the expected ratio for the Sn_2S_6 units. Because $[Sn_2S_6]^{4-}$ anions are stable in FM (as shown by ^{119}Sn solution NMR data) and precipitation of the mesophases is immediate upon addition of the linking metal cations, we expect that they become part of the inorganic framework.

(12) TGA experiments under nitrogen showed the weight loss in a single step corresponding mainly to the degradative removal of the surfactant molecules between 300 and 400 °C. The end product is amorphous by powder XRD. Pyrolysis mass spectrometric analysis showed the emission of ions with m/z 257, on heating at >300 °C. This corresponds to $C_{16}H_{33}S^+$ fragment indicating the abstraction of sulfur atoms from the inorganic framework leading to its collapse.

(13) Pophal, C.; Fuess, H. *Microporous Mesoporous Mater*. **1999**, *33*, 241.

(14) The atomic PDF gives the number of atoms in a spherical shell of unit thickness at a distance r from a reference atom. It peaks at characteristic distances separating correlated pairs of atoms and thus describes the structure of building units. In other words, it shows the inter atomic vectors in the structure and it is a excellent tool at probing local structure regardless of sample crystallinity. The PDF, $G(r) = 4\pi r[\rho(r) - \rho_0]$, is the sine Fourier transform of the total scattering structure function, $S(Q)$, where $\rho(r)$ and ρ_0 are the local and average atomic number densities, respectively, Q is the magnitude

of the wave vector and $S(Q)$ is the corrected and properly normalized total powder diffraction pattern of the material [For details see: Proffen, T.; Billinge, S. J. L. *J. Appl. Crystallogr.* **1999**, *32*, 572. Billinge, S. J. L.; Egami, T. *Phys. Rev. B.* **1993**, *47*, 14 386].
(15) Kennedy, J. D.; McFarlane, W. *Multinuclear NMR*; Mason, J., Ed.; Plenum Press: New York, 1987, pp 305−334. Jiang, T.; Ozin, G. A.; Bedard, R. L. *Adv. Mater*. **1994**, *6*, 860.
(16) In general, the ^{119}Sn NMR chemical shift values decreases with an increase of coordination number. For example, the chemical shift for tetrahedral Sn^{4+} sulfide was found to occur over a range of +70 to −25 ppm; for trigonal bipyramidal Sn^{4+} in the range −300 to −360 ppm and for octahedral Sn^{4+} from 700 to 800 ppm vs Me_4Sn (see ref 15).
(17) The chemical shift for Sn^{4+} in $Na_4Sn_2S_6 \cdot 14H_2O$ occur at 51.3 ppm relative to Me_4Sn with the spinning sidebands extending over ∼800 ppm.
(18) Lippens, P. E. *Phys. Rev.* **1999**, *B60*, 4576.
(19) Rangan, K. K.; Trikalitis, P. N.; Kanatzidis, M. G.; *J. Am. Chem. Soc*. **2000**, *122*, 10 230. Rangan, K. K.; Trikalitis, P. N.; Bakas, T.; Kanatzidis, M. G. *Chem. Commun*. **2001**, 809.
(20) $C_{16}H_{33}NMe_3Br$ possesses no chromophore and shows no PL.
(21) The mesostructured $(CP)_xM_ySn_2S_6$ phases are markedly stable in air over time. Samples that had been hydrothermally posttreated at 100 °C for 12 h showed XRD patterns that were similar to those of as-prepared samples. The thermal stability of these solids was investigated with thermogravimetric analysis (TGA) and pyrolysis mass spectrometry (MS). These compounds show no appreciable weight loss up to 200 °C, suggesting that no solvent molecules are occluded in the structure. Between 200 °C and 400 °C weight loss occurs in two steps due to surfactant decomposition. The inorganic residue at 600 °C was amorphous metal tin sulfide without mesostructured order. Pyrolysis MS at 250 °C of the released volatiles showed a strong peak with m/z 79, which corresponds to the pyridyl headgroup of the surfactant. On further heating, $C_{16}H_{33}S^+$ was detected (m/z = 257) indicating S atom extraction from the framework. This chemical transformation ultimately results in framework collapse.

NL025502K